Parameter Estimation of Vehicle Batteries in V2G Systems: An Exogenous Function-Based Approach

Article *in* IEEE Transactions on Industrial Electronics · September 2021

DOI: 10.1109/TIE.2021.3112980

6 authors, including:

Haris M. Khalid
Higher Colleges of Technology
56 PUBLICATIONS **449** CITATIONS
SEE PROFILE

S M Muyeen
Qatar University
297 PUBLICATIONS **6,125** CITATIONS
SEE PROFILE

M.s. El Moursi
Khalifa University of Science and Technology - Masdar Campus
198 PUBLICATIONS **3,593** CITATIONS
SEE PROFILE

Tha'Er Omar Sweidan
Higher Colleges of Technology
24 PUBLICATIONS **73** CITATIONS
SEE PROFILE

Publication Title: Parameter Estimation of Vehicle Batteries in V2G Systems: An Exogenous Function-Based Approach
Authors: Haris M. Khalid, Farid Flitti, S. M. Muyeen, M. S. El Moursi, Tha'er O. Sweidan, and Xinghuo Yu
 DOI: 10.1109/TIE.2021.3112980

Parameter Estimation of Vehicle Batteries in V2G Systems: An Exogenous Function-Based Approach

Haris M. Khalid, *Member, IEEE*, Farid Flitti, S. M. Muyeen, *Senior Member, IEEE*, M. S. El Moursi, *Senior Member, IEEE*, Tha'er O. Sweidan, and Xinghuo Yu, Fellow, IEEE

***Abstract*—The rapid introduction of electric vehicles (EVs) in the transportation market has initiated the concept of vehicle-to-grid (V2G) technology in smart grids. However, where V2G technology is intended to facilitate the power grid ancillary services, it could also have an adverse effect on the aging of battery packs in EVs. This is due to the instant depletion of power during the charge and discharge cycles, which could eventually impact the structural complexity and electrochemical operations in the battery pack. To address this situation, a median expectation-based regression approach is proposed for parameter estimation of vehicle batteries in V2G systems. The proposed method is built on the property of uncertainty prediction of Gaussian processes for parameter estimation while considering the cell variations as an exogenous function. Firstly, a median expectation-based Gaussian process model is derived to predict the fused and individual cell variations of a battery pack. Secondly, a magnitude-squared coherence model is developed by the error matrix to detect and isolate each variation. This is obtained by extracting the cross-spectral densities for the measurements. The proposed regression-based approach is evaluated using experimental measurements collected from lithium-ion (Li-ion) battery pack in EVs. The parametric analysis of the battery pack has been verified using D-SAT Chroma 8000ATS hardware platform. Performance evaluation shows an accurate estimation of these dynamics even in the presence of injected faults.**

***Index Terms*—Aging analysis, ancillary services, battery degradation, bidirectional charging, electric transportation, electric vehicles (EVs), estimation, grid-to-vehicle, Li-ion batteries, median filter, prediction, recursive, regression, renewable energy, smart grid, vehicle-to-grid.**

Notations: In this paper, a structure is followed to define notations. $\mathbf{E}_{\mu_{1/2}}$ is the median expectation operator. $\mu_{1/2}$ is denoted as the sample size median. A hat over a variable represents an estimate of the variable, e.g. $\hat{\mathcal{I}}$ is an estimate of $\mathcal{I}$. When any of the variables become a function of time, the time index t and its covariates appear as a subscript (e.g. $\mathcal{I}_t$,$\mathcal{I}_{t+1}$,$\mathcal{I}_{t|t}$,$\mathcal{I}_{t|t-1}$).

I. Introduction

THE exhaustion of oil reserves and fossil fuels has alarmed the world with a possibility of source shortage eventually leading to drainage of these natural reservoirs. This has steered us to environmental awareness and devotion to finding clean and sustainable energy resources [1]. In order to promote integration of renewable resources in the energy sector and its support function to provide a clean carbon-free energy, the concept of smart grid has been introduced. Smart grid brings an integrated system of communication and power. It promotes bi-directional communication infrastructure to improve the efficiency, stability and control of optimized power delivery [2].

Recently, EVs have comprehensively contributed towards smart grid by operating in: a) consumer mode, and b) prosumer mode. The consumer mode is implied as grid-to-vehicle (G2V). In G2V technology, EVs behave as an electrical load where the battery charging current is consumed from the utility. The prosumer mode is signified as vehicle-to-grid (V2G). The V2G mode acts as an injecting source where EV participates in obligatory and ancillary services such as demand response (DR) management, peak power supply, power smoothing, voltage stability, etc [3–8]. Note that since the smart grid has essentially no significant storage [9], the operations of generation and transmission have to be simultaneously managed to match the variable load demand.

During the operation of V2G technology, electric drive-based vehicles (EDVs) can generate and feed power to the smart grid. This is due to their property of electric drive motors which are powered by either: 1) a Li-ion battery pack, 2) a fuel cell or a 3) hybrid drive train [10, 11]. The battery-based EVs provide the luxury of charge and discharge functions in ancillary and obligatory services mentioned above. However, to maintain high energy density, Li-ion battery packs comprises hundreds of cells connected in a circuit of series or parallel. This complicated structure becomes more complex when equipped with numerous parametric sensors that are deployed for the measurement of various dynamics such as voltage, temperature, power capacity [12], etc. A sudden variation of these measurements could result in several malfunctions and failures, such as production of combustible gases, thermal runaway [13, 14], etc. To avoid such situations, an effective battery management system (BMS) is required [15–17]. Though BMS has been used to provide function both at component-level and system-level [15, 16, 18], fewer studies have been made about the impact made by grid ancillary services on vehicle battery [19–22]. These studies have focused on practical wear cost model for EVs charge scheduling applications in V2G programs [19], the effect of a vehicle-to-grid (V2G) strategy on the lifetime of different lithium-ion batteries [20], impact of bidirectional charging of V2G technology on commercial li-ion cells used in EVs [21], in-cell variation analysis of vehicle batteries and their impact of propagation with each involved component [22]. The rapid charging and discharging operation of EVs during ancillary services could lead to severe variations and deviations in connections and components of BMS [23]. These variations should be modeled as an exogenous variable to enhance robustness of BMS. Adequate handling while reducing these variations is an essential issue for improving the profile and accuracy of BMS, and thus the motivation of this paper. It is essential to devise a model that could provide resilience towards these variations by system-level identification. A failure to notice these variations could result in amplifying the breakdown of battery-pack.

Therefore, the main contribution in this work is to enhance the parametric access of the vehicle battery pack in a V2G environment. This is obtained by proposing a median-based Gaussian processed regression model to capture the model uncertainty. This is achieved by generating a time series-based recur-

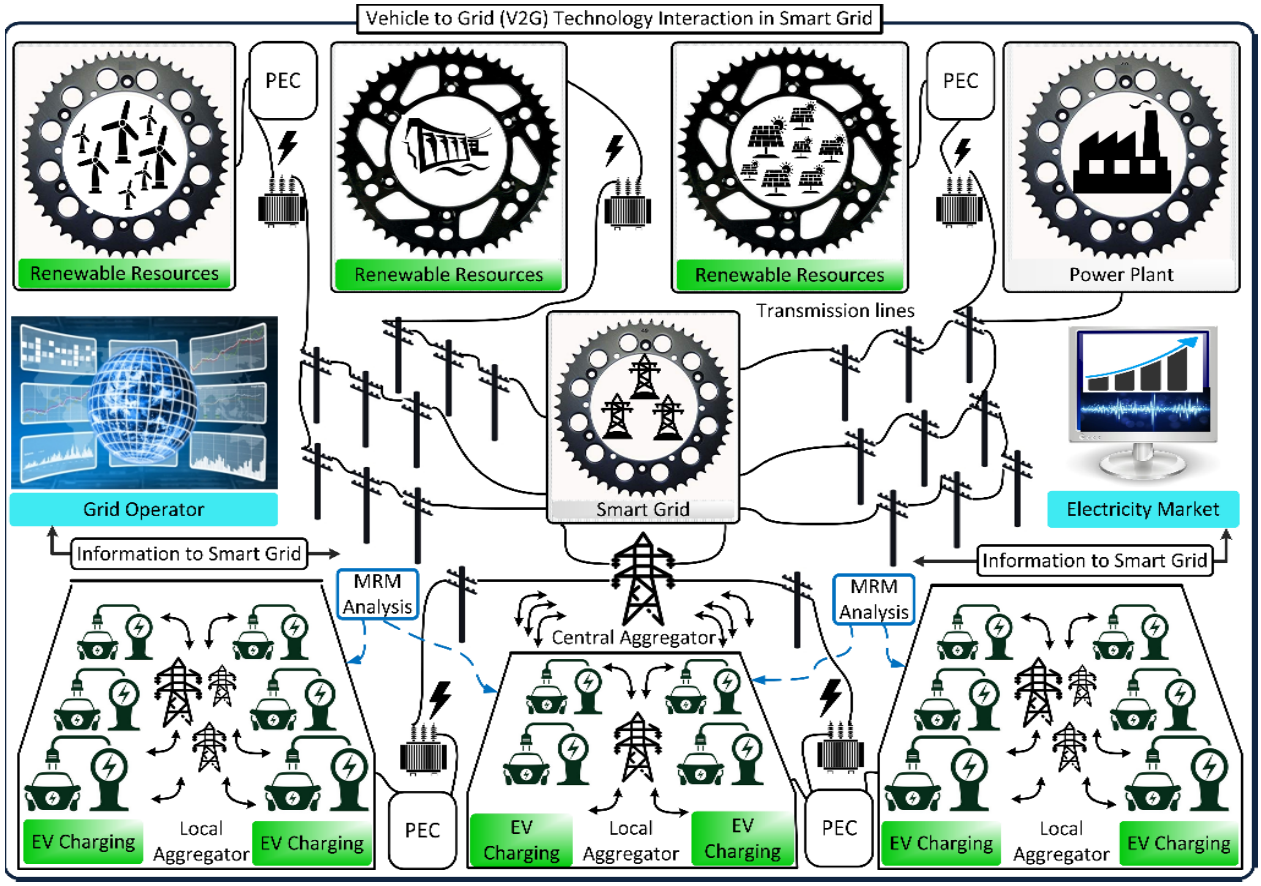

Fig. 1. Vehicle-to-grid technology interaction with smart grid[1]

[1]In this figure, MRM and PEC are the acronyms of median-based regression model approach and power electronics converter respectively.

rence while considering an exogenous regressor function. However, the proposed scheme is not built on an expectation operator which calculates the weighted average between noisy observations and prior measurements [24, 25]. Instead, a fused and individual prediction is calculated by re-deriving median-based expectation. This is to secure the best possible approximation of the true system, while ensuring a better measure of central tendency in the presence of outliers and small sample size.

To understand the methodology of the proposed model into the BMS of EV battery, an overview of the technology setup is represented in Fig. 1. It shows a V2G technology interaction with smart grid through power electronic converter (PEC), where it exploits the energy provided by the indigenous EV communities and is traded to the power grid via management and control of set of local aggregators and a central aggregator. The main ingredients of this duplex power flow between electrical power grid and EV battery are: 1) consumer's EV battery eligible to be utilized for bi-directional energy flow through charging and discharging, 2) communication between the potential consumers and the grid, 3) instant energy management of utility load. The focus of this article is on the analysis[2] of these EV batteries during the V2G interaction with variable consumer load. This is achieved by demonstrating the proposed scheme at a single frequency point, i.e. at a constant operating environment temperature of 20^0C and state-of-health (SOH). Only two parallel cells connected in a thread of series are considered here, which is the standard structure used in Li-ion battery packs [26]. This configuration of each set of two parallel cells is called as the floor.

The formation of paper is as follows: The proposed formulation and scheme is presented in Section II and III respectively. The implementation and evaluation of the scheme is built in Section IV. Finally, conclusion and future work are drawn in Section V. Fig. 2 provides the framework of the paper.

II. Problem Formulation: Cell Variations in a Battery Pack

The problem formulation of cell variations in a battery pack is derived in this section. An overview of the formulation is represented in Fig. 3. Consider a discrete time dynamical model of a battery pack in an EV connected to the grid for providing ancillary services. A standard structure of two-parallel cells connected in a thread of N number of series is considered here [26]. Let the two parallel cells be denoted by $c1$ and $c2$ respectively. Let symbol $\mathcal{C}$ represents the fused form of this configuration, such that $\mathcal{C} = c1 + c2$. The dynamics of each cell are represented by current $\mathcal{I}_t$, temperature $\mathcal{T}_t$, and impedance z_t at time-instant t, such that $t = 0, 1, ..., T$, where T refers to the number of time-instants. A voltage $\mathcal{V}_t$ is supplied to this configuration.

The problem formulation begins with the state representation of current state in (1). This is followed by its observation model in (2). The function of the current state is defined in (3)–(7).

[2] Generally, the analysis of EV batteries is made using battery dynamics, which are modeled using the equivalent circuit models and electro-chemical models for simplicity. However, in this paper, an approximate state space model has been used as a part of parameter estimation scheme. Moreover, in this paper, the electromechanical dynamics of the cells are not considered in the formulation. Instead, cells are considered as conducting bodies only.

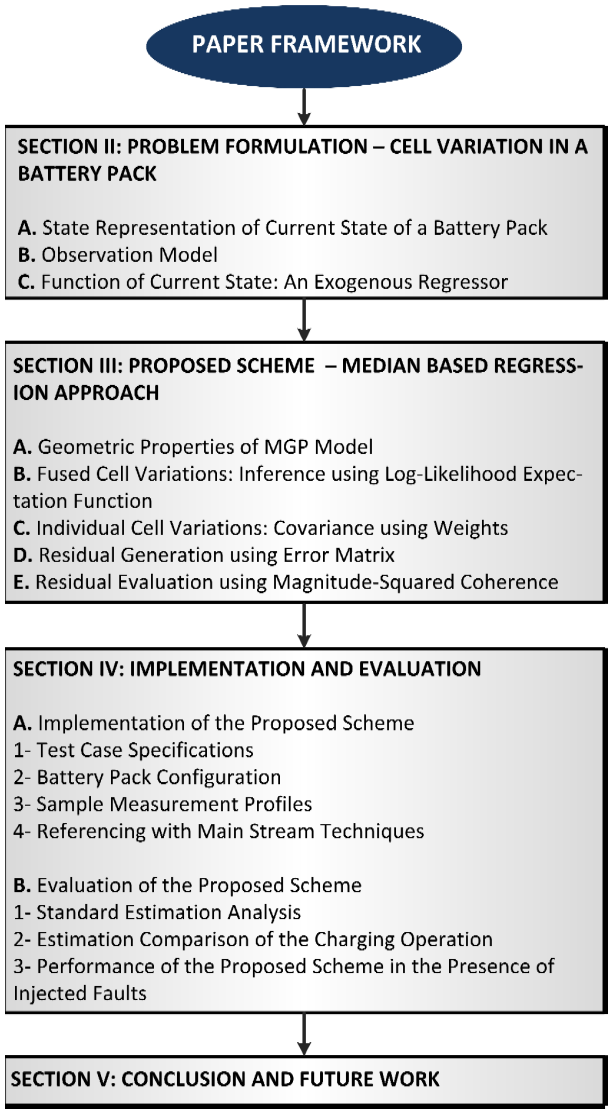

Fig. 2. Framework of the paper

A. State Representation of Current State of a Battery Pack

A state representation of current $\mathcal{I}_t$ of a battery pack can be described as:

$$\mathcal{I}^{\mathcal{C}}_{t+1} = f(\mathcal{I}_{\varepsilon,t})^{\mathcal{C}} + \alpha^{\mathcal{C}}_t \mathcal{T}^{\mathcal{C}}_t + \beta^{\mathcal{C}}_t z^{\mathcal{C}}_t + G^{\mathcal{C}}_t w^{\mathcal{C}}_t \quad (1)$$

where $\mathcal{I}^{\mathcal{C}}_0 \in \mathbf{R}^r$ represents an initial condition of fused current state. Ideally $\mathcal{I}^{\mathcal{C}}_t = \mathcal{I}^{c1}_t + \mathcal{I}^{c2}_t$, such that each individual cell current is the difference between input voltage $\mathcal{V}^{\mathcal{C}}_{1,t}$ and output voltage $\mathcal{V}^{\mathcal{C}}_{2,t}$. This difference is with respect to individual cell impedances as $\mathcal{I}^{c1}_t = \frac{(\mathcal{V}^{\mathcal{C}}_{1,t} - \mathcal{V}^{\mathcal{C}}_{2,t})}{z^{c1}_t}$ and $\mathcal{I}^{c2}_t = \frac{(\mathcal{V}^{\mathcal{C}}_{1,t} - \mathcal{V}^{\mathcal{C}}_{2,t})}{z^{c2}_t}$. Here z^{c1}_t, $z^{c2}_t \in \mathbf{R}^r$ are the impedances of cell $c1$ and $c2$ respectively. $f(\mathcal{I}^{\mathcal{C}}_{\varepsilon,t}) \in \mathbf{R}^r$ is an exogenous regressor function of current state representing dynamic variations in cells. $\alpha^{\mathcal{C}}_t \in \mathbf{R}^{r\times r}$ is the transition matrix of the fused temperature $\mathcal{T}^{\mathcal{C}}_t \in \mathbf{R}^r$. Ideally $\mathcal{T}^{\mathcal{C}}_t = \frac{\mathcal{T}^{c1}_t + \mathcal{T}^{c2}_t}{2}$, such that each individual cell temperature can be stated as: $\mathcal{T}^{c1}_t = \frac{z^{c1}_t}{\alpha^{\mathcal{C}}_t z^{c1}_{0,t}} - \frac{1}{\alpha^{\mathcal{C}}_t} + \mathcal{T}^{c1}_{0,t}$, and $\mathcal{T}^{c2}_t = \frac{z^{c2}_t}{\alpha^{\mathcal{C}}_t z^{c2}_{0,t}} - \frac{1}{\alpha^{\mathcal{C}}_t} + \mathcal{T}^{c2}_{0,t}$. Here $z^{c1}_{0,t}$ and $z^{c2}_{0,t}$ are the standard values of impedance at room temperature $\mathcal{T}^{c1}_{0,t}$ and $\mathcal{T}^{c2}_{0,t}$ respectively. $\beta^{\mathcal{C}}_t \in \mathbf{R}^{r\times r}$ is the transition matrix of impedances z^{c1}_t and z^{c2}_t respectively. Ideally, $z^{\mathcal{C}}_t = z^{c1}_t + z^{c2}_t$, such that each individual cell impedance can be stated as: $z^{c1}_t = z^{c1}_{0,t} + \left[1 + \alpha^{\mathcal{C}}_t(\mathcal{T}^{c1}_t - \mathcal{T}^{c1}_{0,t})\right]$ and $z^{c1}_t = z^{c2}_{0,t} + \left[1 + \alpha^{\mathcal{C}}_t(\mathcal{T}^{c2}_t - \mathcal{T}^{c2}_{0,t})\right]$ respectively. $G^{\mathcal{C}}_t \in \mathbf{R}^{r\times r}$ is the noise transition matrix, which can be defined as a probability vector $p(G_{k,t})$ such that $\sum_{k=1}^{n} p(G_{k,t}) = 1$, where each individual component: 1) is a non-negative real number, 2) must have a probability between 0 and 1 as $0 \leq |p(G_{k,t})| \leq 1$, 3) has sum of all numbers equal to 1. $w^{\mathcal{C}}_t \in \mathbf{R}^r$ is the random process noise.

B. Observation Model

Let the current state of battery pack described in (1) has an observation model at time-instant t as:

$$y^{\mathcal{C}}_t = \mathcal{H}^{\mathcal{C}}_t \mathcal{F}^{\mathcal{C}}_t \mathcal{I}^{\mathcal{C}}_t + v^{\mathcal{C}}_t \quad (2)$$

where $y^{\mathcal{C}}_t \in \mathbf{R}^m$ is the observation output of current state, m is the simultaneous observations for estimations made at time-instant t. $\mathcal{H}^{\mathcal{C}}_t \in \mathbf{R}^{m\times r}$ is the observation matrix and $v^{\mathcal{C}}_t \in \mathbf{R}^m$ is the observation noise. The noises w_t and ν_t are all initially uncorrelated zero-median white Gaussian such that $\mathbf{E}_{\mu_{1/2}}[w_t] = \mathbf{E}_{\mu_{1/2}}[\nu_t] = 0, \forall\, t$. Also $\mathbf{E}_{\mu_{1/2}}[w_p \nu^{'}_q] = 0$ for two instants p and q. Meanwhile, $\mathbf{E}_{\mu_{1/2}}[w_p w^{'}_q] = R_t \delta_{pq}$ when considering the noise process to be a serially uncorrelated, zero-mean, constant, and finite variance process. The variable R_t represents the covariance matrix, and δ_{pq} is a Kronecker delta function used for shifting the integer variable after the presence or absence of noise. Similarly, $\mathbf{E}_{\mu_{1/2}}[\nu_p \nu^{'}_q] = Q_t \delta_{pq}$ with Q_t being the process noise correlation factor.

Once the state and observation model is formulated, function of current state is modeled.

C. Function of Current State: An Exogenous Regressor

The function of current state is represented in the current state model as an exogenous regressor variable, such that $f(\mathcal{I}^{\mathcal{C}}_{\varepsilon,t}) \in \mathbf{R}^r$, It represents dynamic variations in cells for any of its fused form as $\mathcal{C}$, or individual cells $c1$ and $c2$ respectively. $f(\mathcal{I}^{\mathcal{C}}_{\varepsilon,t})$ represents a non-linear mapping function, such that:

$$\mathbf{E}_{\mu_{1/2}}\left[f(\mathcal{I}^{\mathcal{C}}_{\varepsilon,t}) | \mathcal{I}^{\mathcal{C}}_{t+1}\right] = 0 \quad (3)$$

Also, for any two i-th and j-th fused floor of cells,

$$\mathbf{E}_{\mu_{1/2}}\left[f(\mathcal{I}^{\mathcal{C}^i}_{\varepsilon,t}) f'(\mathcal{I}^{\mathcal{C}^j}_{\varepsilon,t})\right] = 0,\ i \neq j \quad (4)$$

where superscript $'$ represents the transpose operator.

Let $f(\mathcal{I}, y, \varepsilon) = g(\mathcal{I}, \varepsilon) - h(\mathcal{I}, y)$, where $g(.)$ and $h(.)$ are non-linear vector functions. The exogenous property satisfies:

$$f(\mathcal{I}^{\mathcal{C}}_{\varepsilon,t}) = \arg \max_{\mathcal{I}^{\mathcal{C}}_{\varepsilon,t} \in \{0,1\}} \mathbf{E}_{\mu_{1/2}}[f(\mathcal{I}, y, \varepsilon) | \mathcal{H}, y] \quad (5)$$

$$= \arg \max_{\mathcal{I}^{\mathcal{C}}_{\varepsilon,t} \in \{0,1\}} \left[\mathbf{E}_{\mu_{1/2}}[g(\mathcal{I}, \varepsilon) | \mathcal{H}, y] - h(\mathcal{I}, y)\right] \quad (6)$$

$$= \begin{cases} 1 \text{ if } \mathbf{E}_{\mu_{1/2}}[g(\mathcal{I}, \varepsilon) | \mathcal{H}, y] - h(1, y) \geq \\ \quad \mathbf{E}_{\mu_{1/2}}[g(0, \varepsilon) | \mathcal{H}, y] - h(0, y) \\ 0\,, \text{Otherwise} \end{cases} \quad (7)$$

Once the exogenous function of current state is modeled on extracted measurements, the proposed scheme is formulated.

III. Proposed Scheme: Median-Based Regression Approach

The proposed scheme is built on the problem formulation. An overview of the framework can be seen in Fig. 3. The geometric properties of median-based Gaussian Process (MGP) model is

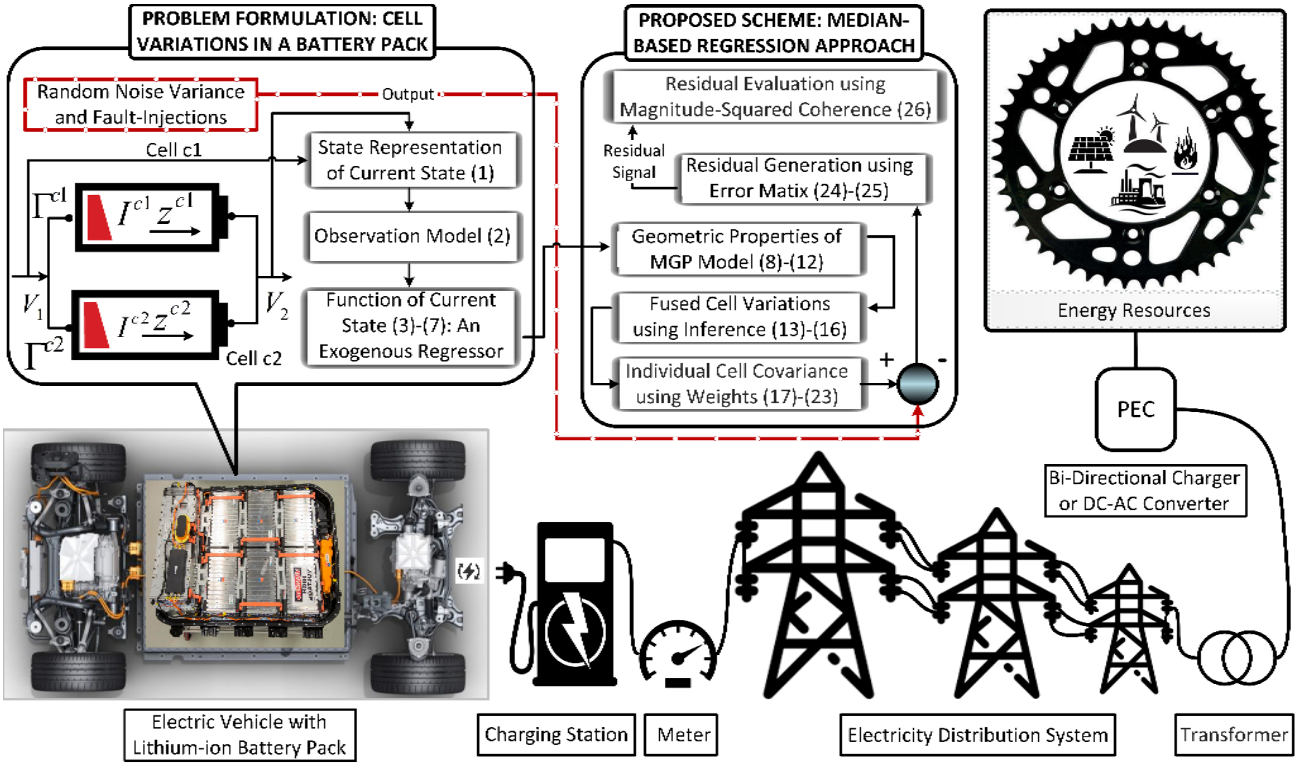

Fig. 3. Formulation framework of the proposed scheme

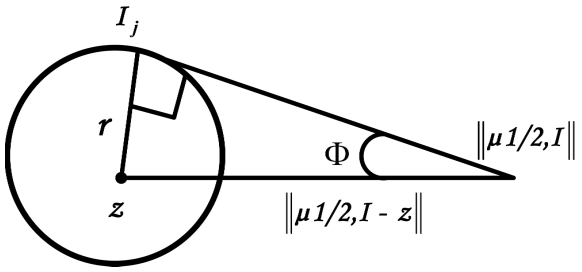

Fig. 4. Median gradient-based convergence diagram

made in (8)–(12). The fused and individual cell variations are derived in (13)–(16) and (17)–(23) respectively. The diagnosis of these variations are made by generating and evaluating the residual at (24)–(25) and (26) respectively.

A. Geometric Properties of MGP Model

The Bayesian inference of the fused current state is made using the MGP model. This requires some additional properties of expectation operator from [18]. Moreover, a realization is required using geometric properties. Let X and Y be two random variables with a Gaussian distribution. The following properties can be stated:

Property 1: If $X, Y \in \mathbf{R}^n$, then $\lim_{X \to Y} \mathbf{E}_{\mu_{1/2}}[|X-Y|^2]=0$.

$$\begin{aligned} p\big(X,Y \le \mu_{1/2}\big) &= p\big(X,Y \ge \mu_{1/2}\big) \\ &= \mathbf{E}_{\mu_{1/2}}\big[(X)^2+(Y)^2-2(X)(Y)\big] \\ &= \Big(\sum_{-\infty}^{\mu_{1/2}} xf(x)\Big)^2 + \Big(\sum_{-\infty}^{\mu_{1/2}} yf(y)\Big)^2 \end{aligned} \tag{8}$$

where $f(x)$ is the probability mass function of X. Simplifying it further, with $f(x)$ to be symmetric gives:

$$\begin{aligned} p\big(X,Y \le \mu_{1/2}\big) &= -2\Big(\sum_{-\infty}^{\mu_{1/2}} xf(x)\Big)\Big(\sum_{-\infty}^{\mu_{1/2}} yf(y)\Big) \\ &= \big(\tfrac{1}{2}\big)^2 + \big(\tfrac{1}{2}\big)^2 - 2\big(\tfrac{1}{2}\big)\big(\tfrac{1}{2}\big) = 0 \end{aligned} \tag{9}$$

The whole process X, Y is called median-square continuous if it is median-square continuous for all $X, Y \in \mathbf{R}^n$.

Property 2: A Guassian process-based function f is said to be median-based differentiable on $\mathbf{R}^r$ if for every sequence $\{X_n\}$ for $i = 1, ..., n$ converges $\|X_n - X\| \to 0$.

Considering the gradient property in [18] and as shown in Fig. 4, let $\mathcal{I}_1, \mathcal{I}_2, \mathcal{I}_3, ..., \mathcal{I}_n \in H$. Also $z \in H$. r is the radius with $\|\mu_{1/2} - z\| > \Phi r$ and $\gamma > 0$. Considering the derivative in the direction of $z - \mu_{1/2}$ for $\dot{f}(X_n)$ gives:

$$\begin{aligned} &\partial f(\mu_{1/2,n}, z-\mu_{1/2,n}) \\ &= \lim_{t \to 0} \frac{f(\mu_{1/2,n} + t(z-\mu_{1/2,n})) - f(\mu_{1/2,n})}{t} \end{aligned} \tag{10}$$

Similarly for the derivative in the direction of $z - \mu_{1/2}$ for $\dot{f}(X)$ gives:

$$\begin{aligned} &\partial f(\mu_{1/2}, z-\mu_{1/2}) \\ &= \lim_{t \to 0} \frac{f(\mu_{1/2} + t(z-\mu_{1/2})) - f(\mu_{1/2})}{t} \end{aligned} \tag{11}$$

Since $\mu_{1/2}$ minimizes the function f, this indicates that:

$$\partial f(\mu_{1/2,n}, z-\mu_{1/2,n}), \partial f(\mu_{1/2}, z-\mu_{1/2}) \ge 0 \tag{12}$$

Based on (10)–(12), $\mathbf{E}_{\mu_{1/2}}[\big(\dot{f}_i(X_n) - \dot{f}_i(X)\big)^2] = 0$ holds.

Note the geometric properties remain the same for symmetric error distributions as well. Once the geometric properties are defined, cell variations are further derived. This is a challenging task due to: 1) prioritizing a data-based approach over a convenient battery model to determine the parametric interactions between cells, 2) introducing a regression property,

and its structural transformation from a conventionally utilized tool for data analysis, forecasting and computer vision to an *a-priori* knowledge-based filter approach, 3) deriving the recursive structure by considering the median-based expectation over the classic weighted average-based expectation.

B. Fused Cell Variations: Inference Using Log-Likelihood Expectation Function

The inference is calculated using the log-likelihood function. This is to get an estimate of unknown parameters of current state as:

$$\begin{aligned}\mathcal{L}(\Theta) &= \log p\big(\mathcal{I}_t^{\mathcal{C}}, f(\mathcal{I}_{\varepsilon,t}^{\mathcal{C}})\big)\\ &= \mathbf{E}_{\mu_{1/2},\mathcal{H}_t|\mathcal{I}_{0,t}^T,y_t} \log p\big(\mathcal{I}_t^{\mathcal{C}}, f(\mathcal{I}_{\varepsilon,t}^{\mathcal{C}})\big)\\ &+ \mathbf{E}_{\mu_{1/2}} \log p\big(f(\mathcal{I}_{\varepsilon,t}^{\mathcal{C}})|\mathcal{I}_t^{\mathcal{C}}\big) \end{aligned} \tag{13}$$

where Θ is the vector of all involved parameters.

The computation of the derivatives of $\mathcal{L}$ with respect to each of the parameters is made as:

$$\begin{aligned}\frac{\partial \mathcal{L}(\Theta)}{\partial \Theta_{\mathcal{I}_t^{\mathcal{C}}, f(\mathcal{I}_{\varepsilon,t}^{\mathcal{C}})}} &= \arg\max_{\mathcal{I}_t} \mathbf{E}_{\mu_{1/2},\mathcal{H}_t|\mathcal{I}_{0,t}^T,y_t} \log p(y_t, \mathcal{H}_t|\mathcal{I}_t)\\ &\quad p(\mathcal{I}_t) + \arg\min_{\mathcal{I}_t^{var}} \big(\mathcal{I}_{t-1}^{var} - \mu_{1,2.t-1}\big)\\ &= \arg\max_{\mathcal{I}_t} \mathbf{E}_{\mu_{1/2},\mathcal{H}_t|\mathcal{I}_{0,t}^T,y_t} \sum_{\mathcal{H}_t\in\Omega} \big(y_t \log(b_t\mathcal{I}_t^{\mathcal{C}})\\ &\quad -\gamma J(\mathcal{I}_t) + \arg\min_{\mathcal{I}_t^{var}} (\mathcal{I}_{t-1}^{var} - \mu_{1/2}, t-1)\\ &= \arg\min_{\mathcal{I}_t} \sum_{\mathcal{H}_t\in\Omega} (b_t\mathcal{I}_t^{\mathcal{C}} - \mathbf{E}_{\mu_{1/2},\mathcal{H}_t|\mathcal{I}_{0,t}^T,y_t} \mathcal{H}_t \log(b_t\mathcal{I}_t^{\mathcal{C}})\\ &\quad +\gamma J(\mathcal{I}_t^{\mathcal{C}}) + \arg\min_{\mathcal{I}_t^{var}} (\mathcal{I}_{t-1}^{var} - \mu_{1/2,t-1}) \end{aligned} \tag{14}$$

where Ω denotes the possible realization of $\mathcal{I}_t^{\mathcal{C}}$. $b_t\mathcal{I}_t^{\mathcal{C}}$ is the realization of the observation matrix $\mathcal{H}_t^{\mathcal{C}}$. J is a positive energy function and γ is a positive parameter.

Taking the difference between (1) and (14) gives the covariance matrix, such that $\mathcal{I}_t^{\mathcal{C}} - \hat{\mathcal{I}}_{t|t-1}^{\mathcal{C}} = P_{t|t-1}^{\mathcal{C}}$. It is presented as:

$$\begin{aligned}P_{t|t-1}^{\mathcal{C}} &= f(\mathcal{I}_{\varepsilon,t}^{\mathcal{C}}) + \alpha_t^{\mathcal{C}}\mathcal{T}_t^{\mathcal{C}} + \beta_t^{\mathcal{C}} z_t^{\mathcal{C}} + G_t^{\mathcal{C}} w_t^{\mathcal{C}} - \arg\min_{I_t^{\mathcal{C}}} \sum_{\mathcal{H}_t^{\mathcal{C}}\in\Omega} (b_t\mathcal{I}_t^{\mathcal{C}})\\ &+ \mathbf{E}_{\mu_{1/2},\mathcal{H}_t|\mathcal{I}_{0,t}^T,y_t} \mathcal{H}_t \log(b_t\mathcal{I}_t^{\mathcal{C}}) - \gamma J(\mathcal{I}_t^{\mathcal{C}})\\ &- \arg\min_{\mathcal{I}_t^{var}} \big(\mathcal{I}_{t-1}^{var} - \mu_{1/2,t-1}\big) \end{aligned} \tag{15}$$

(15) can be further simplified as:

$$\begin{aligned}P_{t|t-1}^{\mathcal{C}} &= \mathcal{F}_t^{\mathcal{C}}\mathcal{I}_t^{\mathcal{C}} - \arg\min_{I_t^{\mathcal{C}}} \sum_{\mathcal{H}_t^{\mathcal{C}}\in\Omega} (b_t\mathcal{I}_t^{\mathcal{C}})\\ &+ \mathbf{E}_{\mu_{1/2},\mathcal{H}_t|\mathcal{I}_{0,t}^T,y_t} \mathcal{H}_t \log(b_t\mathcal{I}_t^{\mathcal{C}}) - \gamma J(\mathcal{I}_t^{\mathcal{C}}) + f(\mathcal{I}_{\varepsilon,t}^{\mathcal{C}})\\ &(\alpha_t^{\mathcal{C}}\mathcal{T}_t^{\mathcal{C}} + \beta_t^{\mathcal{C}} z_t^{\mathcal{C}}) - \arg\min_{\mathcal{I}_t^{var}} (\mathcal{I}_{t-1}^{var} - \mu_{1/2,t-1}) + G_t^{\mathcal{C}} w_t^{\mathcal{C}} \end{aligned} \tag{16}$$

The covariance matrix $P_{t|t-1}^{\mathcal{C}}$ is derived here using the innovation process and first principles. However, it is assumed here that both cells have the same dynamics, which is not the situation since the individual cell dynamics are dependent on: 1) the position of cells in the array of pack, 2) heat dissipation, and 3) load handling of cells. This gives motivation to derive the covariance representing the individual cell variations of floor of cells.

C. Individual Cell Variations: Covariance using Weights

The individual cell covariance can be represented by assigning weights among the parallel connection. Let Ψ_t^{c1} and Ψ_t^{c2} be the assigned weights for cells $c1$ and $c2$ respectively. This makes the presentation of $\hat{\mathcal{I}}_{t|t}^{\mathcal{C}}$ as:

$$\begin{aligned}\hat{\mathcal{I}}_{t|t}^{\mathcal{C}} &= P_{t|t}^{\mathcal{C}}\Big(\Psi_t^{c1} {P_{t|t}^{c1}}^{-1}\big[\alpha_t^{\mathcal{C}}\mathcal{T}_t^{c1}\beta_t^{\mathcal{C}} z_t^{c1} b_t f(\mathcal{I}_{\varepsilon,t}^{\mathcal{C}})(\mathcal{I}_{t-1}^{var}\\ &\quad - \mu_{1/2,t-1})\big] + \Psi_t^{c2} {P_{t|t}^{c2}}^{-1}\big[\alpha_t^{\mathcal{C}}\mathcal{T}_t^{c2}\beta_t^{\mathcal{C}} z_t^{c2} b_t f(\mathcal{I}_{\varepsilon,t}^{\mathcal{C}})\\ &\quad (\mathcal{I}_{t-1}^{var} - \mu_{1/2,t-1})\big]\Big) \end{aligned} \tag{17}$$

where the difference between $\hat{\mathcal{I}}_t^{c1}$ and $\hat{\mathcal{I}}_t^{c2}$ can be expressed by $\zeta_t^{\mathcal{C}}$ as follows:

$$\zeta_t^{\mathcal{C}} = \hat{\mathcal{I}}_{t|t}^{c1} - \hat{\mathcal{I}}_{t|t}^{c2} \tag{18}$$

The expression (18) can be normalized further. This is done by using median-based expectation operator as:

$$\begin{aligned}\mathbf{E}_{\mu_{1/2}}\big[\zeta_t^{\mathcal{C}}\zeta_t^{\mathcal{C}}{}'\big] &= \mathbf{E}_{\mu_{1/2}}\big[\hat{\mathcal{I}}_{t|t}^{c1} - \mathcal{I}_{t|t}^{\mathcal{C}} - (\hat{\mathcal{I}}_{t|t}^{c2} - \mathcal{I}_{t|t}^{\mathcal{C}})\big]\big[\hat{\mathcal{I}}_{t|t}^{c1}\\ &\quad - \mathcal{I}_{t|t}^{\mathcal{C}} - (\hat{\mathcal{I}}_{t|t}^{c2} - \mathcal{I}_{t|t}^{\mathcal{C}})\big]' \end{aligned} \tag{19}$$

and is equivalent to:

$$\mathbf{E}_{\mu_{1/2}}[\zeta_t^{\mathcal{C}}\zeta_t^{\mathcal{C}}{}'] = P_{I,t|t}^{c1} + P_{I,t|t}^{c2} - P_{I,t|t}^{\mathcal{C}} - P_{I,t|t}^{\mathcal{C}'} \tag{20}$$

Using the calculation from (17) to (20), the weighted matrices for cells $c1$ and $c2$ can be expressed in closed-form as:

$$\psi_t^{c1} = \frac{\Big(\frac{\hat{\mathcal{I}}_{t|t}^{\mathcal{C}}}{P_{t|t}^{\mathcal{C}}} - \psi_t^{c2} {P_{t|t}^{c2}}^{-1}\big[\alpha_t^{\mathcal{C}}\mathcal{T}_t^{c2}\beta_t^{\mathcal{C}} z_t^{c2} b_t f(\mathcal{I}_{\varepsilon,t}^{\mathcal{C}})\Xi\big]\Big)}{{P_{t|t}^{c1}}^{-1}\big[\alpha_t^{\mathcal{C}}\mathcal{T}_t^{c1}\beta_t^{\mathcal{C}} z_t^{c1} b_t f(\mathcal{I}_{\varepsilon,t}^{\mathcal{C}})\Xi\big]} \tag{21}$$

$$\psi_t^{c2} = \frac{\Big(\frac{\hat{\mathcal{I}}_{t|t}^{\mathcal{C}}}{P_{t|t}^{\mathcal{C}}} - \psi_t^{c1} {P_{t|t}^{c1}}^{-1}\big[\alpha_t^{\mathcal{C}}\mathcal{T}_t^{c1}\beta_t^{\mathcal{C}} z_t^{c1} b_t f(\mathcal{I}_{\varepsilon,t}^{\mathcal{C}})\Xi\big]\Big)}{{P_{t|t}^{c2}}^{-1}\big[\alpha_t^{\mathcal{C}}\mathcal{T}_t^{c2}\beta_t^{\mathcal{C}} z_t^{c2} b_t f(\mathcal{I}_{\varepsilon,t}^{\mathcal{C}})\Xi\big]} \tag{22}$$

where $\Xi = (\mathcal{I}_{t-1}^{var} - \mu_{1/2,t-1})$.

Considering (21) and (22), the covariance matrix for fused current state can be stated as:

$$\begin{aligned}P_{t|t}^{\mathcal{C}} &= \hat{I}_{t|t}^{\mathcal{C}}\Big(\frac{\hat{\mathcal{I}}_{t|t}^{\mathcal{C}}}{P_{t|t}^{\mathcal{C}}} - \psi_t^{c2} {P_{t|t}^{c2}}^{-1}\big[\alpha_t^{\mathcal{C}}\mathcal{T}_t^{c2}\beta_t^{\mathcal{C}} z_t^{c2} b_t f(\mathcal{I}_{\varepsilon,t}^{\mathcal{C}})\Xi\big]\\ &+ \frac{\hat{\mathcal{I}}_{t|t}^{\mathcal{C}}}{P_{t|t}^{\mathcal{C}}} - \psi_t^{c1} {P_{t|t}^{c1}}^{-1}\big[\alpha_t^{\mathcal{C}}\mathcal{T}_t^{c1}\beta_t^{\mathcal{C}} z_t^{c1} b_t f(\mathcal{I}_{\varepsilon,t}^{\mathcal{C}})\Xi\big]\Big)\\ &= \hat{I}_{t|t}^{\mathcal{C}}\Big(\frac{2\hat{\mathcal{I}}_{t|t}^{\mathcal{C}}}{P_{t|t}^{\mathcal{C}}} - \mathcal{P}_{t|t}^{c1} - \mathcal{P}_{t|t}^{c2}\Big) \end{aligned} \tag{23}$$

where $\mathcal{P}_{t|t}^{c1} = \psi_t^{c1} {P_{t|t}^{c1}}^{-1}\big[\alpha_t^{\mathcal{C}}\mathcal{T}_t^{c1}\beta_t^{\mathcal{C}} z_t^{c1} b_t f(\mathcal{I}_{\varepsilon,t}^{\mathcal{C}})\Xi\big]$, and $\mathcal{P}_{t|t}^{c2} = \psi_t^{c2} {P_{t|t}^{c2}}^{-1}\big[\alpha_t^{\mathcal{C}}\mathcal{T}_t^{c2}\beta_t^{\mathcal{C}} z_t^{c2} b_t f(\mathcal{I}_{\varepsilon,t}^{\mathcal{C}})\Xi\big]\Big)$ represents the covariance matrices for cell $c1$ and $c2$ respectively. Note the covariance matrices of temperature, impedance and voltage can also be calculated using the state representation and the relationships of (1) and (2).

The output of the individual cell will determine the residual generation.

D. Residual Generation using Error Matrix

The generated residual e_{res} is usually calculated to detect any 1) unusual dynamic variations, 2) biased signatures, and 3) system-faults. Considering cell $c1$ these variations can be detected as:

$$\begin{aligned}e_{\text{res},y,t}^{c1} &= \mathcal{H}_t^{c1} e_{\mathcal{I},t+1}^{c1}\\ &= H_t\big(\mathcal{F}_t^{c1} - [\mathbf{E}_{\mu_{1/2}}\mathcal{I}_{t+1}^{c1}(y_t^{c1} - v_t)']R_{e,t}^{-1}\mathcal{H}_t^{c1}\big) \end{aligned}$$

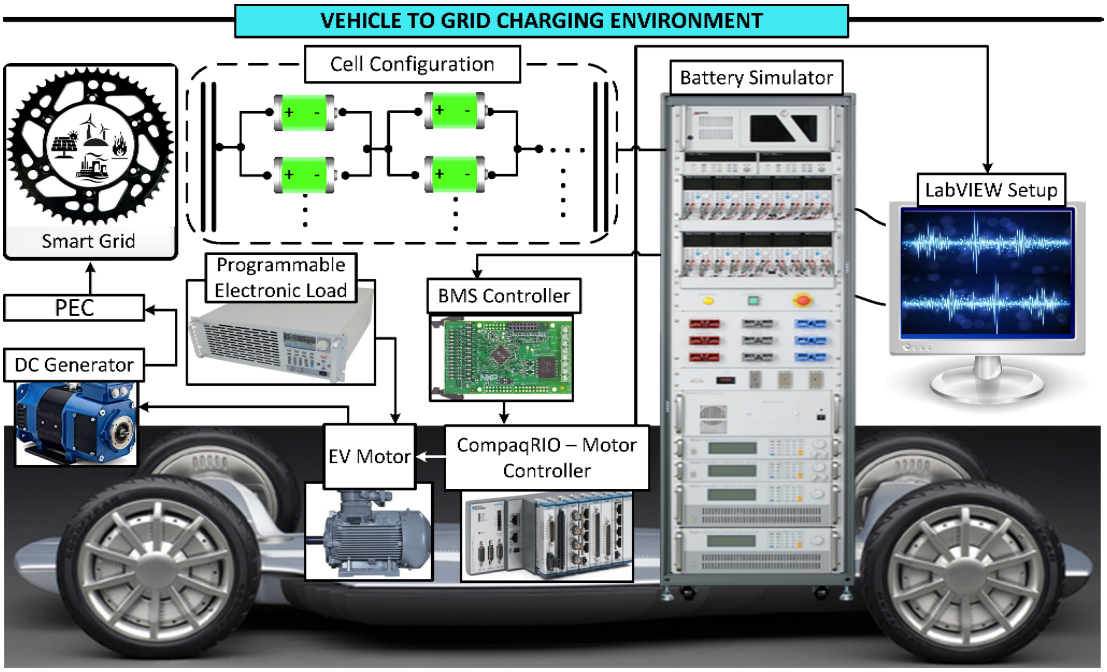

Fig. 5. Setup for V2G bi-directional charging system

$$(\mathcal{I}_t^{c1} - \hat{\mathcal{I}}_t^{c1}) + \Xi[\xi_t f(y_t^{c1}, \mathcal{I}_t^{c1}) - \xi_{f,t} f(y_t^{c1}, \mathcal{I}_t^{c1})] \quad (24)$$

where $\mathcal{F}_t^{c1} \in \mathbf{R}^{r \times r}$ is the modal matrix of the exogenous function, $R_{e,t}$ is the covariance of observation noise having a zero-mean multivariate normal distribution $\mathcal{N}$, such that $R_{e,t}$: $v_t \sim \mathcal{N}(0, R_{e,t})$, $f(y_t^{c1}, \mathcal{I}_t^{c1}) \in \mathbf{R}^r$ is a non-linear vector function of y_t^{c1} and $\mathcal{I}_{c1}$. $\xi_t, \xi_{f,t} \in \mathbf{R}$ are the parameters that shows a change due to fault-injection f.

The generated residual is asymptotically convergent when the parameters show no change due to the injected fault, such that ξ_t, $\xi_{f,t}$, $\lim_{t\to\infty} e_{\text{res},y,t}^{c1} = 0$, where the difference between residual generation can be represented by a Lyapunov variable $\mathcal{V}$, such that:

$$\begin{aligned} \Delta\mathcal{V} &= \mathbf{E}_{\mu_{1/2}}\left[\mathcal{V}(e_{\mathcal{I},t+1} | e_{\mathcal{I},t}, \mathcal{I}_t^{c1} - \hat{\mathcal{I}}_t^{c1})\right] \\ &\leq -e_{\text{res},y,t}^{c1} \aleph_t e_{\mathcal{I},t}^{c1} + 2\|(e_{\text{res},y,t}^{c1}\| \| R_{e,t} \xi_{f,t} | \mathcal{V} \| e_{\mathcal{I},t}^{c1}\| \\ &\leq -\rho \|e_{\text{res},y,t}^{c1}\|^2 - \mathcal{V}(e_{\text{res},y,t}^{c1}) \\ &< 0 \end{aligned} \quad (25)$$

where ρ is defined to minimize the positive definite matrix $\aleph_t$.

Once the residual is computed, the evaluation of residual is made.

E. Residual Evaluation using Magnitude-Squared Coherence

The evaluation of residual requires a selection of threshold to determine a false data injection. This was made using test statistic Γ_{stat} computed by magnitude-squared coherence as:

$$\Gamma_{\text{stat}} = \frac{|S_t S_{f,t}|^2}{S_t^2 S_{f,t}^2}, \begin{cases} \leq \eta_{th} \text{ no attack} \\ > \eta_{th} \text{ attack} \end{cases} \quad (26)$$

where S_t and $S_{f,t}$ are the cross-spectral densities of fault-free and fault-injected parameters respectively. η_{th} is a computed threshold value. Note that the threshold value is chosen to ensure a low false alarm probability during the course of an accurate residual evaluation.

Once the formulation has been defined, the pseudo code is represented for the implementation.

Algorithm 1 Pseudo code of the proposed schemes

$N \rightarrow$ number of series,
$T \rightarrow$ number of time-instants,
$SP \rightarrow$ state representation,
$OM \rightarrow$ observation model,
$CSF \rightarrow$ current state function,
$GP \rightarrow$ geometric properties,
$MGP \rightarrow$ median-based gaussian process filter,
$FCV \rightarrow$ fused cell variation,
$ICC \rightarrow$ individual cell covariance,
$RG \rightarrow$ residual generation,
$RE \rightarrow$ residual evaluation,
for i=1 to N
    $\boldsymbol{SP}_i \leftarrow$measurements($\boldsymbol{N}_i$);
    $\boldsymbol{OM}_i \leftarrow$measurements($\boldsymbol{N}_i$);
    $\boldsymbol{CSF}_i \leftarrow$extract($\boldsymbol{SP}_i$,$\boldsymbol{OM}_i$);
end for
for i=1 to N
    $\boldsymbol{FCV}_i \leftarrow$median-expectation($\boldsymbol{GP}_i$);
end for
for i=1 to N
    $\boldsymbol{ICC}_i \leftarrow$median-expectation($\boldsymbol{GP}_i$);
end for
for$i$=1 to N
    $\boldsymbol{MGP}_i \leftarrow$estimation-performance(***Residual-Generation***$_i$);
    $\boldsymbol{MGP}_i \leftarrow$estimation-performance(***Residual-Evaluation***$_i$);
end for
Parametric-Estimation$\leftarrow$extract(***SP***,***OM***)
Residual$\leftarrow$extract(***SP***,***OM***)
Threshold$\leftarrow$extract(***SP***,***OM***)

F. Summary of Pseudo Code Representation:

The proposed method built on MGP filter for parametric estimation can also be transformed into a pseudo code as seen in Al-

gorithm 1. The variables used in the code are defined from Line 1 to 11. A *for loop* is applied for assigning measurements to state representation and observation model, followed by extraction of model from the measurements for current state function, median expectation for fused cell variation, median expectation for individual cell covariance, residual generation and residual evaluation. These loops can be seen in Line 12 to 16, 17 to 19, 20 to 22, and 23 to 26 respectively. The calculation of parametric estimates, residual, and threshold are extracted in Line 27–29.

IV. Implementation and Evaluation

A. Implementation of the Proposed Scheme

The proposed scheme was implemented[3] on a Li-ion battery pack of an EV. It was further evaluated by conducting test case-based experiments which were performed using the guidelines issued by the United States Department of Energy battery test manual [27, 28]. The evaluation was conducted under different operating conditions. The evaluated profiles of battery-pack analysis were further verified using D-SAT Chroma 888 ATS hardware platform.

1) Test Case Specifications: The test case designed for this implementation and evaluation can be seen in Fig. 5. It represents a V2G bi-directional charging environment, which is composed of: 1) a D-SAT Chroma battery cell simulator, which comprises of 2160 KWh of charging capacity, 2) an NXP BMS controller, 3) a DC motor, 4) a labVIEW-based compaqRIO controller (for DC motor), 5) a DC generator, 6) a boost DC-DC converter, which contains a resonant circuit for a soft-switching and operation, 7) a programmable electronic load, 8) a data acquisition unit, which is utilized for collecting measurement signals, 9) data storage, and 10) a computer, which is required for controlling the current load and supply.

2) Battery Pack Configuration: The battery pack configuration considered for this test case is a floor combination of four sets of parallel cells which are connected in a string of series. Each battery cell has a nominal capacity of 2.3 Ah and a nominal voltage of 3.2 V.

3) Sample Measurement Profiles: The sample measurement profile of the cells connected in this configuration are plotted in Fig. 6, where Fig. 6(a)–(c) shows the standard plots of voltage, temperature, and total current respectively. The sampled current profile during charging operation of a duty cycle is shown in Fig. 6(d).

4) Referencing with Main Stream Techniques: Since, the proposed scheme is built on a recursive structure, it is referenced as follows. Firstly, it is referenced with mainstream techniques of 1) EKF [29, 30], and 2) UKF [31]. Secondly, it is referenced with [22] for highlighting the property of exogenous regressor. Thirdly, it is referenced comprehensively with other regression methods [32–34]: 1) linear regressions, 2) standard Gaussian processes, 3) support vector machine (SVM), 4) neural networks (NN), 5) regression trees, 6) boosted trees, and 7) bagged trees. The later are regression methods, and they are not originally designed to estimate the current variations on the floor of cells in a battery pack.

[3] The test was conducted with a frequency of 10 Hz at 20 ^{0}C. The implementation was tested offline because of: 1) an injected fault, and 2) other sensitive battery parameters. These reasons could challenge the performance of BMS leading to system shutdown and other potential damages. Note that the focus of this paper is to make pack-level analysis of vehicle batteries in V2G systems.

B. Evaluation of the Proposed Scheme

The objective of this study is to evaluate the estimation performance of the proposed scheme.

1) Standard Estimation Analysis: A standard estimation analysis was conducted on cell $c2$ and voltage V_2 supplied to the floor of cells $c3$ and $c4$ respectively. The idea is to analyze the initial performance of the proposed scheme towards handling the individual cell dynamics without an external injection. An estimation comparison of cell $c2$ current measurement between the mainstream EKF, UKF, and the proposed median-based regression approach is made. Fig. 6(e)–(g) shows the zoomed version of the sets highlighted in black rectangular boxes. It can be seen that there is a huge over-shoot spike at the beginning of the current profile and a delayed sag from 5.6 h–10.1 h. This required an abrupt initialization procedure to estimate these variations. All the techniques performed reasonably well. However, EKF started the tracking slowly in the initial time windows. This is due to its linear property of calculating the difference between the state and its estimate at every iteration. This was not the case with UKF which performed reasonably well. However, the proposed scheme gives more accurate results than both EKF and UKF. This was due to its Gaussian processes-based Bayesian inference system. Similarly, an estimation comparison of voltage V_2 measurement between [22] and the proposed scheme is made. Fig. 6(h)–(k) shows the zoomed version of the sets outlined in black rectangular boxes. Both techniques performed well. However, the proposed scheme took lead in 6h–11h by capturing the model uncertainty and providing more access to instant dynamic variations.

2) Estimation Comparison of the Charging Operation: An estimation comparison of the charging operation is also made with seven regression methods. The profile of Fig. 6(h) was considered for this comparison without any external injection. Since the regression methods work on the concept of curve-fitting to best fit the series of data-points, the data-set is divided into two subsets for testing and training purposes. This is also due to their property of learning the relationship between several independent or particular variables and a set of dependent variables. The two subsets are: 1) a data-set of first 9 h for training the regressors, 2) a sample of remaining 11 h for testing the measurements. Fig. 7(a)–(f) and Fig. 7(g)–(l) show the phases of train-fit and test-fit respectively. Here Fig. 7(a) shows the full profile of train-fit. Fig. 7(b)–(f) shows the zoomed version of the sets of the same training profile outlined in black rectangular boxes. Fig. 7(g)-(l) shows the phases of test-fit. Fig. 7 (g) shows the full profile of test-fit. Fig. 7(h)-(l) shows the zoomed version of sets of full test-fit profile. Note the data analysis and forecasting property of the proposed scheme is built on a recursive engine, and it does not require any training and testing of best fit. Instead, it estimates using the *a-priori* knowledge of time sequence. Generally, all the techniques show very good fits during the training phase. However, linear regression per-

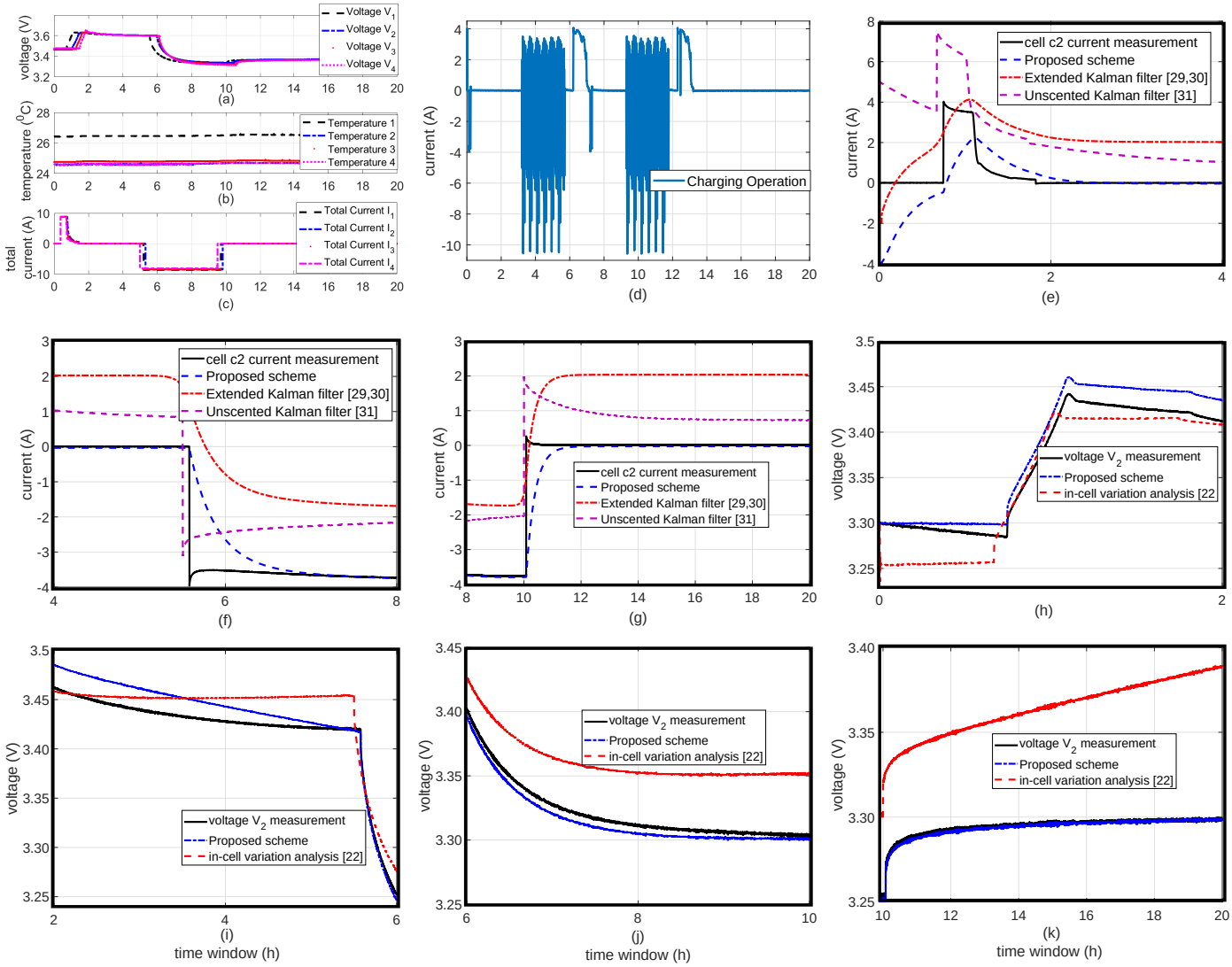

Fig. 6. Measurements of a) voltage, b) temperature, and c) total current. d) Sample current profile during charging operation of a duty cycle. (e–g) Zoomed version of various phases of the current estimates for cell $c2$. (h–k) Zoomed version of various phases of the estimates for voltage V_2.

formed the least with apparent misfits in the zoomed windows of Fig. 7(b)-(f). One can specifically notice at 0.17 h in Fig. 7(b) and 7.5 h–8.3 h in Fig. 7(f) that linear regression failed to estimate the sharp transitions with a misfit that reaches up to 12 A. Less prominent misfits of approximately 0.5 A are also visible around 0.07 h in Fig. 7(b). The misfits are due to the linear nature of the regression technique which utilizes the least square for these situations. The shortcoming of this utilization is that it could not hold the situation with complex I/O relationships. On the contrary, the performance of the remaining regression methods was quiet decent especially during the quasi-periodic variations in Fig. 7(d) and (e). This was due to their non-linear nature of the structure. Bagged trees have their test performances deteriorated in the test fit (See Fig. 7(b)–(f)). The trees showed spikes that reached 0.4 A–0.9 A for very low values of the individual cell variation. Similarly, neural networks (NN) also showed apparent misfits in the test phase. Despite of a feedback forward structure utilized with a back propagation algorithm to optimize the network, the misfit for NN reached up to 0.3 A. This could be due to the dependency on the training data-set with less adaptivity towards sparse representation of an instant variation. In contrast, the proposed scheme was fast enough to capture all the variations.

3) Performance of the Proposed Scheme in the Presence of Injected Faults: Once a fault-free standard analysis was made, a test case was developed to evaluate the performance in the presence of injected faults. On the top of dynamic variations of duty cycle of current profile, three data-injection scenarios are included as follows: 1) an added energy variation at 12.3 h–13.2 h, 2) A spike variation at 15.0 h–16.0 h, 3) a random noise injection at 16.8 h–19.1 h. All these injections can be seen in Fig. 7 (m). An estimation comparison of cell variation in the presence of fault-injection is made with the regression methods. The comparison was made using the mean-square error (MSE). The profile comparison of all the methods can be seen in Fig. 7(n). The low performance of linear regression compared to other methods is expected as it represents the least complex model among all tested techniques. After linear regression, bagged trees and NN showed the most inconsistent performances with increased MSEs in the testing window. The

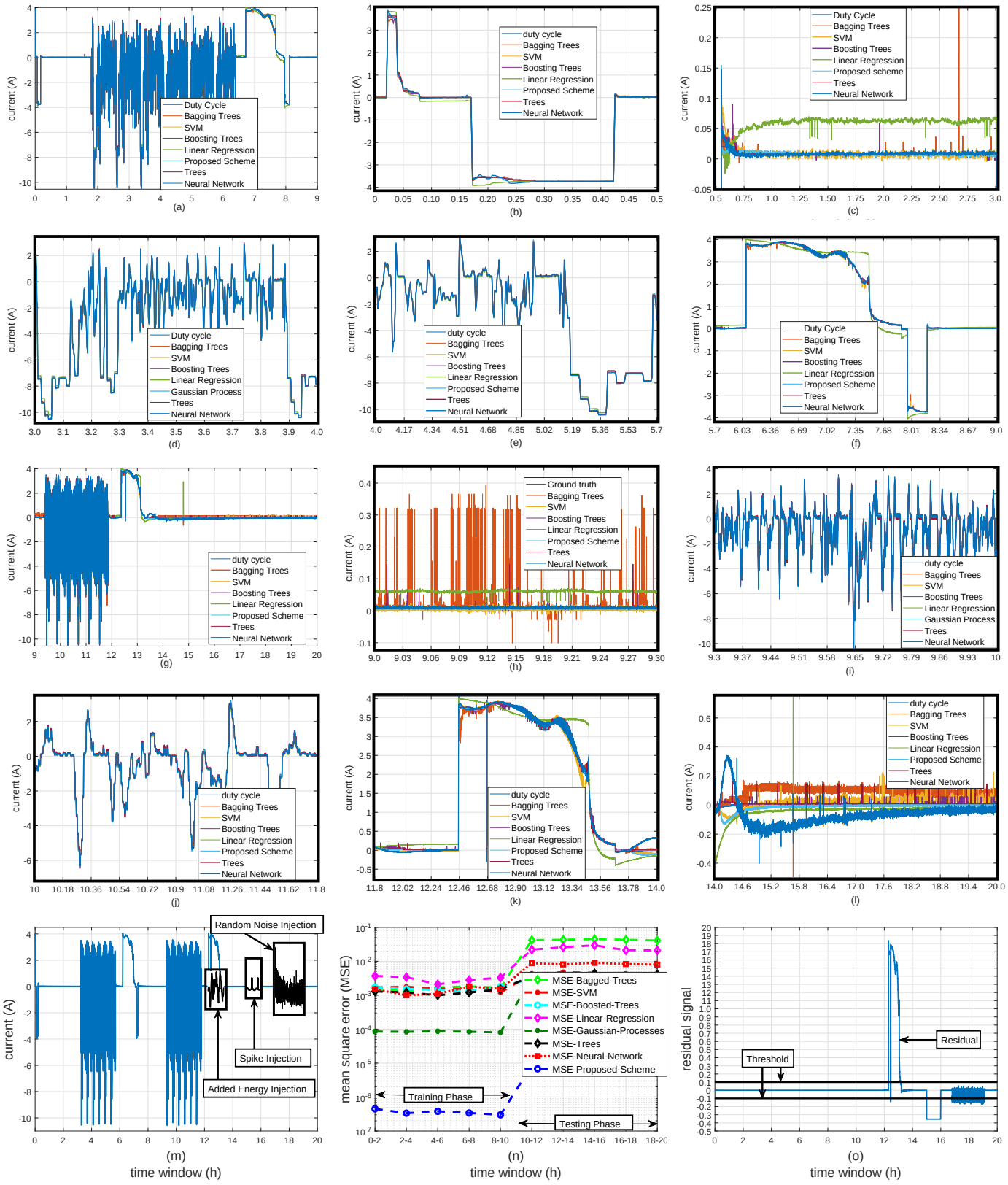

Fig. 7. (a) Training data-set for estimation of cell variations for 0 h–9 h. (b–f) Zoomed version of various phases of the estimated training data-set. (g) Testing data-set estimation of cell variations for 11 h–20 h. (h–l) Zoomed version of various phases of the estimated testing data-set. m) Fault injections in current duty cycle, n) its MSE comparison, and o) Evaluation of residual signal.

performance obtained with bagging may be explained by the fact that bagging technique relies on randomly sampling the training data-set to train tree regressors. NN test performance degradation may be explained by its limitation towards overfit-

ting. Trees and SVM have also shown a minor degradation in their test performances. Boosted trees achieved the most consistent performances with almost similar MSE for training and testing. Similarly, Gaussian Processes method also showed a decent performance for both training and test. However, there is notable difference between its training and test phase. On the contrary, the proposed scheme was consistent with high accuracy in both windows. Due to its recursive structure, it also did not require any training or testing. Furthermore, injected fault evaluation has been made by structuring a residual vector between fault-free and faulty profile of current charging operation. This is achieved by generating the error matrix and magnitude-squared coherence. The injected faults were detected and evaluated properly as shown in Fig. 7(0). The threshold selected for the residual was $\pm$ 0.1.

V. Conclusion and Future Work

In this paper, the cell variations of a vehicle battery involved in V2G technologies have been analyzed with a parameter estimation approach. This is achieved by considering these variations as an exogenous regressor. The proposed median expectation-based Gaussian process model is built on this concept to estimate the fused and individual cell variations in the floor of arrays of cells while improving the service life of the battery packs in battery-based EVs. To enhance the analysis of these variations at local level, the Bayesian inference-based structure is supported by an error matrix-based residual vector and a magnitude-square coherence model. The proposed scheme has been demonstrated to eventually uplift the effectiveness of duplex power flow in power grid ancillary services. Estimation comparison of the scheme has been made with the existing mainstream techniques of automotive Li-ion batteries as well as with the standard regression methods.

In the future, studies will be conducted to quantitatively analyze the aging analysis of these battery packs and their structural impact on the fused and individual cell dynamics. Moreover, methods to support near real-time estimation for deploying preventive maintenance of battery packs will be proposed.

References

[1] A. Ipakchi and F. Albuyeh, "Grid of the future," *IEEE Power and Energy Magazine*, vol. 7, no. 2, pp. 52–62, Mar./Apr. 2009.

[2] I. S. Bayram, M. Z. Shakir, M. Abdullah, and K. Qaraqe, "A survey on energy trading in smart grid," *IEEE Global Conference on Signal and Information Processing*, pp. 258–262, Atlanta, GA, USA, 3–5 Dec. 2014.

[3] R. A. Raustad, "The role of V2G in the smart grid of the future," *Interface*, vol. 24, no. 1, pp. 53–60, Jan. 2015.

[4] G. Wenzel, M. Pincetic, D. Olivares, J. MacDonald, D. Callaway, "Real-time charging strategies for EV aggregator to provide ancillary services," *IEEE Trans. Smart Grid*, vol. 9, no. 5, pp. 5141–5151, Sep. 2018.

[5] K.-W. Hu, P.-H. Yi, and C.-M. Liaw, "An EV SRM drive powered by battery/supercapacitor with G2V and V2H/V2G capabilities," *IEEE Trans. Industrial Electronics*, vol. 62, no. 8, pp. 4714–4727, Aug. 2015.

[6] U. K. Madawala, and D. J. Thrimawithana, "A bidirectional inductive power interface for electric vehicles in V2G systems," *IEEE Trans. Industrial Electronics*, vol. 58, no. 10, pp. 4789–4796, Oct. 2011.

[7] R. Sioshansi,P. Denholm, "The value of plug-in hybrid electric vehicles as grid resources," *The Energy Journal*, vol. 31, no. 3, pp. 1–23, Jul. 2010.

[8] X. Wang and Q. Liang, "Energy management strategy for plug-in hybrid electric vehicles via bi-directional vehicle-to-grid," *IEEE Systems Journal*, vol. 11, no. 3, pp. 1789–1798, Sep. 2017.

[9] D. Lindley, "Smart grids: The energy storage problem," *Nature*, vol. 463, pp. 18–20, Jan. 2010.

[10] K. R. Reddy, S. Meikandasivam, "Load flattening and voltage regulation using PHEV's storage capacity with vehicle prioritization using ANFIS," *IEEE Trans. Sustainable Energy*, vol. 11, no. 1, pp. 260–270, Jan. 2020.

[11] S. Xia, S. Q. Bu, X. Luo, K. W. Chan, and X. Lu, "An autonomous real-time charging strategy for plug-in electric vehicles to regulate frequency of distribution system with fluctuating wind generation," *IEEE Trans. Sustainable Energy*, vol. 9, no. 2, pp. 511–524, Apr. 2018.

[12] M. Armand, and J. -M. Tarascon, "Building better batteries," *Nature*, vol. 451, pp. 652–657, Feb. 2008.

[13] L. Su, J. Zhang, C. Wang, Y. Zhang, Z. Li, Y. Song, T. Jin, Z. Ma, "Identifying main factors of capacity fading in li-ion cells using orthogonal design of experiments," *Applied Energy*, vol. 163, pp. 201–210, Feb. 2016.

[14] S. J. Harris, D. J. Harris, and C. Li, "Failure statistics for commercial lithium ion batteries: A study of 24 pouch cells," *Journal of Power Sources*, vol. 342, pp. 589–597, Feb. 2017.

[15] B. G. Carkhuff, P. A. Demirev, R. Srinivasan, "Impedance-based battery management system for safety monitoring of li-ion batteries," *IEEE Trans. Industrial Electronics*, vol. 65, no. 8, pp. 6497–6504, Aug. 2018.

[16] D. F. Frost, D. A. Howey, "Completely decentralized active balancing BMS," *IEEE Trans. Power Electronics*, vol. 33, no. 1, pp. 729–738, Jan. 2018.

[17] R. Xiong, Y. Zhang, J. Wang, H. He, S. Peng, and M. Pecht, "Li-ion battery health prognosis based on a real battery management system used in electric vehicles," *IEEE Trans. Vehicular Technology*, vol. 68, no. 5, pp. 4110–4121, May 2018.

[18] H. M. Khalid, Q. Ahmed and J. C.-H. Peng, "Health monitoring of li-ion battery systems: A median expectation-based diagnosis approach (MEDA)," *IEEE Trans. Transportation Electrification*, vol. 1, no. 1, pp. 94–105, Jul. 2015.

[19] H. Farzin, M. F. Firuzabad, and M. M. Aghtaie, "A practical scheme to involve degradation of li-ion batteries in vehicle-to-grid applications," *IEEE Trans. Sustainable Energy*, vol. 7, no. 4, pp. 1730–1738, Oct. 2016.

[20] A. Marongiu, M. Roscher, and D. Sauer, "Influence of the V2G strategy on the aging behavior of li-ion battery EVs," *Applied Energy*, vol. 137, pp. 899–912, Jan. 2015.

[21] M. Dubarry, A. Devie, M. Katherine, "Durability and reliability of EV batteries under electric utility grid operations: Bidirectional charging impact analysis," *Journal of Power Sources*, vol. 358, pp. 39–49, Aug. 2017.

[22] H. M. Khalid, and J. C. -H. Peng, "Bi-directional charging in V2G systems: An in-cell variation analysis of vehicle batteries," *IEEE Systems Journal*, vol. 14, no. 3, pp. 3665–3675, Sep. 2020.

[23] G. Rancilio, "Battery energy storage systems for ancillary services provision," *Thesis*, Department of Energy, Politecnico Di Milano, pp. 1154, Mar. 2018.

[24] M. S. Grewal, V. Henderson, R. Miyasako, "Application of Kalman filtering to the calibration and alignment of inertial navigation systems," *IEEE Trans. Automatic Control*, vol. 36, no. 1, pp. 4–14, Jan. 1991.

[25] H. Hijazi, and L. Ros, "Joint data QR-detection and Kalman estimation for OFDM time-varying Rayleigh channel complex gains," *IEEE Trans. Communication*, vol. 58, no. 1, pp. 170–178, Jan. 2010.

[26] A. C.-Arenas, S. Onori, G. Rizzoni, "A control-oriented li-ion battery pack model for PHEV cycle-life studies and system design with consideration of health management," *Journal of Power Sources*, vol. 279, pp. 791–808, Apr. 2015.

[27] J. Marcicki, M. Canova, M., A. T. Conlisk, and G. Rizzoni, "Design and parametrization analysis of a reduced-order electrochemical model of graphite/$LiFePO_4$ cells for SOC/SOH estimation," *Journal of Power Sources*, vol. 237, pp, 310–324, Sep. 2013.

[28] "Battery test manual for PHEVs," *U.S. Dept. Ener.*, Mar. 2008.

[29] A. Singh, A. Izadian, and S. Anwar, "Adaptive nonlinear model-based fault diagnosis of li-ion batteries," *IEEE Trans. Industrial Electronics*, vol. 62, no. 2, pp. 1002–1011, Jul. 2014.

[30] H. He, R. Xiong, X. Zhang, F. Sun, and J. Fan, "State-of-Charge estimation of the li-ion battery using an adaptive extended Kalman filter based on an improved Thevenin model," *IEEE Trans. Vehicular Technology*, vol. 60, no. 4, pp. 1461–1469, May 2011.

[31] H. Hea, R. Xiong, and J. Peng, "Real-time estimation of battery SOC with unscented Kalman filter and RTOS μCOS-II platform," *Applied Energy*, vol. 162, pp. 1410–1418, Jan. 2016.

[32] D. J. C. MacKay, "Information theory, inference and learning algorithms," *Cambridge Uni. Press*, pp. 1–640, New York, NY, USA, 2002.

[33] S. Haykin, "Neural Networks: A comprehensive foundation," *Prentice Hall*, pp. 1–842, Upper Sddle River, New Jersey, 1999.

[34] J. S. Taylor and N. Cristianini, "Kernel methods for pattern analysis," *Cambridge Uni. Press*, pp. 1–462, 2004.

AUTHORS BIOGRAPHY

Haris M. Khalid (M'13–SM'20) received the B.S. (Hons.) degree in Mechatronics and Control Systems Engineering from the University of Engineering and Technology (UET), Lahore, Pakistan, in 2007, and the M.S. and Ph.D. degrees in control systems engineering from the King Fahd University of Petroleum and Minerals (KFUPM), Dhahran, Saudi Arabia, in 2009 and 2012, respectively.

He is currently an Assistant Professor in electrical and electronics engineering with the Higher Colleges of Technology (HCT), Sharjah, UAE. He has also served as an Applied Research Coordinator in Sharjah Campuses of HCT. In 2012, he joined the Distributed Control Research Group, KFUPM, as a Research Fellow. From 2013-2016, he was a Research Fellow with the Power Systems Research Laboratory, the *i*Center for Energy, Masdar Institute (MI), Khalifa University (KU), Abu Dhabi, UAE, which is an MI-MIT Cooperative Program with the Massachusetts Institute of Technology (MIT), Cambridge, MA, USA. During this tenure, he was also a Visiting Scholar with the Energy Systems, Control, and Optimization Lab, ADNOC Research and Innovation Center, KU. He has authored/coauthored more than 60 peer-reviewed research publications. He has served as an Energy Specialist in UAE Space Agency "Tests in Orbit" Competitions, which are partnered with Dream-Up and Nano-Racks. His research interests include power systems, cyber-physical systems, electric vehicles, signal processing, V2G technology, fault diagnostics, filtering, estimation, and condition monitoring.

Dr. Khalid is an active Technical Chair of IEEE-ASET 2018–2022 (seven group of conferences) organized in UAE. He is also a Reviewer for the IEEE TRANSACTIONS ON POWER SYSTEMS, IEEE TRANSACTIONS ON NEURAL NETWORKS AND LEARNING SYSTEMS, IEEE TRANSACTIONS ON CONTROL OF NETWORK SYSTEMS, IEEE TRANSACTIONS ON TRANSPORTATION ELECTRIFICATION, and IEEE SYSTEMS JOURNAL. He is the Associate Editor of Frontiers in Energy Research | Smart Grid. He is the Associate Editor of Frontiers in Energy Research | Smart Grid. He is a Fellow of Advance HE UK.

F. Flitti received the M.Eng. degree in automatic control and signal processing from Paris-Sud University, Paris, France, in 2002, and the Ph.D. degree in computer vision and image processing from Louis Pasteur University, Strasbourg, France, in 2005.

He is currently an Assistant Professor in electrical and electronics engineering with the Higher Colleges of Technology (HCT), Dubai, UAE. He held two postdoctoral research positions in the Hong Kong University of Science and Technology, Hong Kong, and the University of Western Australia, Perth, WA Australia. He was also principal scientist in the R&D group at BHP Billiton, Perth, Australia for five years. He has authored/coauthored more than 30 peer-reviewed research publications. His research interests include computer vision, Marko models, pattern recognition, machine learning and their applications. Dr. F. Flitti is serving as reviewer for many international journals and conferences. He has also served in the technical committees for DELTA 2008 and ASET 2018-2020.

S. M. Muyeen (*S*'03–M'08–SM'12) received the B.Sc. (Eng.) degree from the Rajshahi University of Engineering and Technology, Rajshahi, Bangladesh, formerly known as the Rajshahi Institute of Technology, in 2000, and the M.Eng. and Ph.D. degrees from the Kitami Institute of Technology, Kitami, Japan, in 2005 and 2008, respectively, all in electrical and electronic engineering.

He is currently a Full Professor with the Department of Electrical Engineering, Qatar University, Doha, 2713, Qatar. He has authored/coauthored more than 250+ articles in different journals and international conferences and also six books as an author or editor. His research interests include power system stability and control, electrical machine, flexible ac transmission system, energy storage system, renewable energy, and HVdc system.

Dr. Muyeen is serving as Editor/Associate Editor for many prestigious journals from IEEE, IET, and other publishers including IEEE TRANSACTIONS OF SUSTAINABLE ENERGY, IEEE POWER ENGINEERING LETTERS, IET Renewable Power Generation, IET Generation, Transmission & Distribution, etc. He has been a Keynote Speaker and an Invited Speaker at many international conferences, workshops, and universities. He is a Fellow of Engineers Australia.

Mohamed Shawky El Moursi (M'12, SM15) received the B.Sc. and M.Sc. degrees from Mansoura University, Mansoura, Egypt, in 1997 and 2002, respectively, and the Ph.D. degree from the University of New Brunswick (UNB), Fredericton, NB, Canada, in 2005, all in electrical engineering.

He was a Research and Teaching Assistant in the Department of Electrical and Computer Engineering, UNB, from 2002 to 2005. He joined McGill University as a Postdoctoral Fellow with the Power Electronics Group. He joined Vestas Wind Systems, Arhus, Denmark, in the Technology R&D with the Wind Power Plant Group. He was with TRANSCO, UAE, as a Senior Study and Planning Engineer. He is currently a Professor in the Electrical and Computer Engineering Department at Khalifa University of Science and Technology- Masdar Campus and seconded to a Professor Position in the Faculty of Engineering, Mansoura University, Mansoura, Egypt and currently on leave. He was a Visiting Professor at Massachusetts Institute of Technology, Cambridge, Massachusetts, USA. Dr. Shawky is currently an Editor of IEEE Transactions on Power Delivery, IEEE Transactions on Power Systems, Associate Editor of IEEE Transactions on Power Electronics, Associate Editor of IEEE Transactions on Smart Grid, Guest Editor of IEEE Transactions on Energy Conversion, Guest Editor-in-Chief for special section between TPWRD and TPWRS, Editor for IEEE Power Engineering Letters, Regional Editor for IET Renewable Power Generation and Associate Editor for IET Power Electronics Journals. His research interests include power system, power electronics, FACTS technologies, VSC-HVDC systems, Microgrid operation and control, Renewable energy systems (Wind and PV) integration and interconnections.

Tha'er O. Sweidan received his B.Sc.in Electrical Engineering from the Hashemite University, Jordan in 2011 and M.Sc. in Electrical Power Engineering from the Yarmouk University, Jordan in 2015. Currently He is an Engineering Instructor in electrical engineering with the Higher Colleges of Technology (HCT), Sharjah, UAE. He had joined Electrical Engineering Department in the Hashemite University in Jordan as lab Instructor from 2012 to 2018. His current research interests include power systems and electrical machines dynamics, electric vehicles, renewable energy systems and battery management systems.

Xinghuo Yu (M'92-SM'98-F'08) received BEng and MEng degrees in Electrical and Electronic Engineering from the University of Science and Technology of China, Hefei, China, in 1982 and 1984, and PhD degree in Control Science and Engineering from Southeast University, Nanjing, China in 1988, respectively.

He is an Associate Deputy Vice-Chancellor, a Distinguished Professor, and a Vice-Chancellor's Professorial Fellow at Royal Melbourne Institute of Technology (RMIT University), Melbourne, Australia. He was the President of IEEE Industrial Electronics Society for 2018 and 2019. His research interests include control systems, complex and intelligent systems, and smart energy systems. He has served as an Associate Editor of IEEE Transactions on Automatic Control, IEEE Transactions on Circuits and Systems I: Regular Papers, IEEE Transactions on Industrial Electronics and IEEE Transactions on Industrial Informatics. He received a number of awards and honors for his contributions, including 2013 Dr.-Ing. Eugene Mittelmann Achievement Award of IEEE Industrial Electronics Society, 2018 M A Sargent Medal from Engineers Australia and 2018 Australasian AI Distinguished Research Contribution Award from Australian Computer Society.